Journal of Experimental Botany, Vol. 69, No. 5 pp. 1183–1197, 2018
doi:10.1093/jxb/erx474 Advance Access publication 21 December 2017
This paper is available online free of all access charges (see http://jxb.oxfordjournals.org/open_access.html for further details)

RESEARCH PAPER

Improved chloroplast energy balance during water deficit enhances plant growth: more crop per drop

Keshav Dahal* and Greg C. Vanlerberghe†

Department of Biological Sciences and Department of Cell and Systems Biology, University of Toronto Scarborough, 1265 Military Trail, Toronto, Ontario, M1C1A4 Canada

* Present address: Fredericton Research and Development Centre, Agriculture and Agri-Food Canada, 850 Lincoln Road, PO Box 20280, Fredericton, New Brunswick, E3B 4Z7 Canada

† Correspondence: gregv@utsc.utoronto.ca

Received 23 November 2017; Editorial decision 7 December 2017; Accepted 7 December 2017

Editor: Tracy Lawson, University of Essex, UK

Abstract

The non-energy-conserving alternative oxidase (AOX) respiration of plant mitochondria is known to interact with chloroplast photosynthesis. This may have consequences for growth, particularly under sub-optimal conditions when energy imbalances can impede photosynthesis. This hypothesis was tested by comparing the metabolism and growth of wild-type *Nicotiana tabacum* with that of AOX knockdown and overexpression lines during a prolonged steady-state mild to moderate water deficit. Under moderate water deficit, the AOX amount was an important determinant of the rate of both mitochondrial respiration in the light and net photosynthetic CO_2 assimilation (*A*) at the growth irradiance. In particular, AOX respiration was necessary to maintain optimal proton and electron fluxes at the chloroplast thylakoid membrane, which in turn prevented a water-deficit-induced biochemical limitation of photosynthesis. As a result of differences in *A*, AOX overexpressors gained more biomass and knockdowns gained less biomass than wild-type during moderate water deficit. Biomass partitioning also differed, with the overexpressors having a higher percentage, and the knockdowns having a lower percentage, of total above-ground biomass in reproductive tissue than wild-type. The results establish that improving chloroplast energy balance by using a non-energy-conserving respiratory electron sink can increase photosynthesis and growth during prolonged water deficit.

Keywords: CO_2 assimilation, energy balance, growth, mitochondrial alternative oxidase, photosynthesis, respiration, thylakoid membrane proton circuit, water deficit.

Introduction

Photosynthesis and respiration represent the core of carbon and energy metabolism, and hence are key determinants of growth (Stitt *et al.*, 2010; Millar *et al.*, 2011). However, these metabolic systems may experience energy imbalances, such as a mismatch between supply and demand for ATP and/or NAD(P)H. Such imbalances may have consequences for overall plant performance (Hüner *et al.*, 1998; Wilson *et al.*, 2006; De Block and Van Lijsebettens, 2011). In photosynthesis, the absorption of light energy by chloroplast thylakoid pigments drives the generation of ATP and NADPH, which

Abbreviations: *A*, net CO_2 assimilation rate; AOX, alternative oxidase; CET, cyclic electron transport; cyt, cytochrome; DIRK, dark-interval relaxation kinetics; DW, dry weight; ECS, electrochromic shift; ETR, rate of linear electron transport through photosystem II; g_{H^+}, conductance of the thylakoid membrane to proton movement from lumen to stroma; g_s, stomatal conductance to CO_2; iWUE, instantaneous leaf water use efficiency; LET, linear electron transport; NPQ, non-photochemical-energy quenching; ΔpH, chemical potential; Δψ, electrical potential; PPFD; photosynthetic photon flux density; PSI, photosystem I; PSII, photosystem II; pmf, proton motive force; R_D, rate of mitochondrial respiration in the dark; R_L, rate of mitochondrial respiration in the light; RWC, relative water content; qP, photochemical energy quenching; *T*, transpiration rate; v_{H^+}, relative rate of proton flux from stroma to lumen; WT, wild-type.

are used by the Calvin cycle to produce triose phosphates through the assimilation of CO_2. However, owing to factors such as a highly variable light environment and availability of CO_2, photosynthesis is prone to energy imbalances (Kramer and Evans, 2011). For example, reduced availability of CO_2 during water deficit, due to stomatal closure, reduces the consumption of ATP and NADPH being generated by the thylakoid reactions (Lawlor, 2002; Flexas *et al.*, 2004).

In plant mitochondria, the respiratory electron transport chain is branched, such that electrons from ubiquinol can flow to cytochrome (cyt) oxidase (via Complex III and cyt *c*) or the alternative oxidase (AOX) (Finnegan *et al.*, 2004; Plaxton and Podestá, 2006; Noctor *et al.*, 2007; Millar *et al.*, 2011). Electron flow to AOX bypasses two of three sites of proton translocation across the inner mitochondrial membrane. While this reduces the ATP yield of the respiratory chain, it also allows NAD(P)H turnover to continue, even when energy charge (ATP/ADP) is high (Vanlerberghe *et al.*, 1995). Such flexibility may prevent an over-reduction of respiratory chain components that can otherwise result in the generation of reactive oxygen and nitrogen species (Maxwell *et al.*, 1999; Cvetkovska and Vanlerberghe, 2012; Alber *et al.*, 2017).

The impact of AOX respiration on overall growth remains poorly understood (Vanlerberghe, 2013). In theory, AOX could negatively impact growth since growth requires ATP and AOX reduces the ATP yield of respiration. On the other hand, this energy cost might be outweighed by beneficial impacts of AOX, perhaps related to maintaining energy balance. Several studies, including those using mutant or transgenic lines, have investigated the link between AOX respiration and growth. These studies have yielded conflicting results, with both positive and negative impacts of AOX on growth being reported (Millar *et al.*, 1998; Millenaar *et al.*, 2001; Fiorani *et al.*, 2005; Sieger *et al.*, 2005; Florez-Sarasa *et al.*, 2007; Mathy *et al.*, 2010; Skirycz *et al.*, 2010; Chai *et al.*, 2012; Zidenga *et al.*, 2012). Hence, AOX remains a component of primary metabolism whose impact on growth remains elusive (Gifford, 2003; Noctor *et al.*, 2007; Lawlor and Tezara, 2009; Amthor, 2010; Nunes-Nesi *et al.*, 2011). Since AOX gene expression and protein amount often increase in response to abiotic and biotic stresses, these might be conditions where the pathway is particularly beneficial (Clifton *et al.*, 2006). Computational models predict increased AOX respiration with increases in irradiance, a prediction based on the ability of AOX to aid in the maintenance of energy balance during photosynthesis (Buckley and Adams, 2011; Cheung *et al.*, 2015; Nikoloski *et al.*, 2015).

The chloroplast itself is well-equipped with mechanisms to balance ATP and NAD(P)H supply by the thylakoid reactions with ATP and NADPH use by the Calvin cycle and other chloroplast metabolism (Oelze *et al.*, 2008; Kramer and Evans, 2011; Foyer *et al.*, 2012; Schöttler *et al.*, 2015; Wobbe *et al.*, 2016; Foyer *et al.*, 2017). In thylakoid membranes, transfer of light energy to photosystem II (PSII) and photosystem I (PSI) drives electron transport to generate NADPH. Electron transport is coupled to proton translocation from stroma to lumen, generating a proton motive force (pmf) across the thylakoid membrane with both chemical potential (ΔpH) and electrical potential ($\Delta\psi$) components. This pmf is used by the thylakoid membrane-localized ATP synthase to drive the synthesis of ATP. The total pmf can be composed of variable fractions of ΔpH and $\Delta\psi$, both of which are equally effective at driving ATP synthesis. However, ΔpH also has important roles in the regulation of photosynthesis and maintenance of energy balance. A lower lumen pH supports the generation of non-photochemical energy quenching (NPQ) and slows electron flux through the cyt b_6f complex (Cruz *et al.*, 2005; Foyer *et al.*, 2012; Tikhonov, 2014). Given this dual role of lumen protons to both support ATP synthesis and regulate photosynthesis, the proton circuit between stroma and lumen must be tightly and flexibly regulated, in order to optimize photosynthesis in response to changing metabolic and environmental conditions. It is thus a central regulatory feature of chloroplast metabolism (Kramer *et al.*, 2003; Cruz *et al.*, 2005; Kohzuma *et al.*, 2009; Tikhonov, 2013; Armbruster *et al.*, 2017; Shikanai and Yamamoto, 2017). Nonetheless, it is recognized that extra-chloroplast metabolism, including mitochondrial metabolism, is also required to optimize photosynthesis (Krömer, 1995; Hoefnagel *et al.*, 1998; Raghavendra and Padmasree, 2003; Noguchi and Yoshida, 2008; Taniguchi and Miyake, 2012; Tcherkez *et al.*, 2012; Gardeström and Igamberdiev, 2016). The details of these beneficial chloroplast–mitochondrial interactions are less well understood.

We previously showed that, in response to a rapid onset of water deficit stress, the severity of which increased continually over time, the AOX amount in *Nicotiana tabacum* leaf was a strong determinant of the rate of respiration in the light (R_L) (Dahal *et al.*, 2014; Dahal and Vanlerberghe, 2017). In turn, R_L strongly influenced short-term photosynthetic performance. Here, we show that increased AOX respiration is also an important acclimation to a prolonged steady-state moderate water deficit. We show that AOX respiration improves net CO_2 assimilation rate (A) by promoting energy balance in the chloroplast, in particular by staving off changes in the thylakoid proton circuit that otherwise culminate in a biochemical limitation of photosynthesis. Finally, we show that the long-term increase in A promoted by AOX respiration improves growth under water deficit.

Materials and methods

Plant material, growth conditions, and experimental design

Wild-type (WT) and transgenic *Nicotiana tabacum* cv. Petit Havana were used. Plant lines B7 and B8 have elevated amounts of AOX protein due to the presence of an *AOX1a* transgene driven by a constitutive promoter, while plant lines RI9 and RI29 have suppressed amounts of AOX protein due to the presence of an *AOX1a* RNA interference construct. All are independent transgenic lines homozygous for their transgene (Wang *et al.*, 2011; Wang and Vanlerberghe, 2013; Cvetkovska *et al.*, 2014; Dahal and Vanlerberghe, 2017). A key objective was to subject plants to a reasonably steady-state and moderate degree of water deficit throughout their growth period. This would allow a comparison of the plant lines under conditions where they had become well acclimated to a long-term moderate water deficit (Harb *et al.*, 2010).

Seeds were germinated in vermiculite at room temperature and low light. For each independent experiment, tiny seedlings (16 d after sowing) were transplanted into four large rectangular pots (74 cm long, 23 cm wide, 23 cm deep). Each pot contained five seedlings (one each of WT, B8, B7, RI9, and RI29) equally spaced along the length of the pot. The order of plant lines along the length of the pot was randomized across the four pots. Each pot contained an equivalent weight of dry growing medium (8.8 kg) that was saturated to field capacity with water (12.1 litres) prior to transplanting. The growing medium had four parts soil (Pro-mix BX, Premier Horticulture, Rivière-du-Loup, Canada) and one part vermiculite. The pots were placed in growth chambers (model PGC-20, Conviron, Winnipeg, Canada) with 16 h photoperiod, temperature of 28 °C/22 °C (light/dark), relative humidity of 60% and photosynthetic photon flux density (PPFD) of 700 µmol m^{-2} s^{-1} (700 PPFD).

Preliminary experiments with WT plants established a watering schedule (see Supplementary Fig. S1 at *JXB* online) that allowed the seedlings to become established, while also consistently generating plants in which the relative water content (RWC) of leaf 5 was approximately 82% by day 23 in the growth chamber (Supplementary Fig. S2A). Since well-watered tobacco normally maintain a RWC closer to 90%, the day 23 plants were experiencing what we have previously characterized as mild water deficit (Dahal and Vanlerberghe, 2017). Following the established watering schedule then resulted in a gradual decline in RWC to approximately 71% by day 33, characterized as moderate water deficit (Dahal and Vanlerberghe, 2017). Following this, the watering schedule generated plants where RWC remained relatively stable (fluctuating between 66 and 72%) through day 50 (Supplementary Fig. S2A). Throughout this time course, leaf RWC correlated closely with soil water content (Supplementary Fig. S2B). In experiments comparing the different plant lines, an identical watering schedule was used, and most of the physiological and biochemical analyses (see below) were performed at days 23, 33, 39, and 45 after transplanting. Since some of these analyses required destructive sampling, one of the four pots was used at each time point, within each independent experiment. In these experiments, soil water content averaged 86% on day 23, and then ranged from 57 to 63% on the other days (Supplementary Fig. S2D).

Gas exchange and Chl a fluorescence

Leaf CO_2 exchange and Chl *a* fluorescence from PSII were measured in the growth chamber using a portable system (GFS-3000; Heinz Walz, Effeltrich, Germany). Gas exchange data were used to calculate A, transpiration rate (T) and stomatal conductance (g_s) (von Caemmerer and Farquhar, 1981; Farquhar and Sharkey, 1982). Instantaneous leaf water use efficiency (iWUE) was calculated as A/T (Condon *et al.*, 2004; Bernacchi and VanLoocke, 2015). Gas exchange was also used to evaluate respiration. Respiration rate in the dark (R_D) was measured following a 30 min dark pre-incubation. R_L was estimated by the Kok method as previously described (Dahal *et al.*, 2014).

Simultaneous gas exchange and Chl *a* fluorescence analyses followed a dark pre-incubation of 30 min. Minimum fluorescence (F_o), maximal fluorescence in the dark-adapted leaf (F_m) or light-adapted leaf (F_m'), steady state fluorescence in the light-adapted leaf (F_s), and minimal fluorescence in the light-adapted leaf (F_o') were used to calculate photosynthetic parameters (Maxwell and Johnson, 2000). The maximal quantum yield of PSII (F_v/F_m) was calculated as $(F_m–F_o)/F_m$ and the effective quantum yield or operating efficiency of PSII (Φ_{PSII}) was calculated as $(F_m'-F_s)/F_m'$ (Genty *et al.*, 1989). The rate of linear electron transport (LET) through PSII (ETR) was calculated as ETR=(Φ_{PSII}×PPFD×0.5 × 0.84) where 0.84 and 0.5 represent estimates that leaves absorb 84% of incident photons and that 50% of these are absorbed by PSII (Yamori *et al.*, 2011*a*). Photochemical energy quenching (qP) was calculated using the puddle model where qP=$(F_m'-F_s)/(F_m'-F_o')$ (Kramer *et al.*, 2004). The fraction of closed (reduced) PSII reaction centers, known as excitation pressure, was calculated as 1−qP. NPQ, a measure of heat dissipation of absorbed light energy, was calculated as $(F_m–F_m')/F_m'$ (Maxwell and Johnson, 2000). Light response curves were measured at intervals over the range of 0–2000 PPFD (from low to high PPFD, 6 min at each irradiance) and CO_2 concentration of 400 µmol mol^{-1}.

Leaf absorption spectroscopy

A DUAL-PAM-100 measuring system (Heinz Walz) equipped with DUAL-E and DUAL-DB modules were used to simultaneously measure PSI absorbance and PSII fluorescence. Absorbance changes were used to estimate the rate of electron transport through PSI (Klughammer and Schreiber, 2008), while fluorescence changes were used to estimate ETR through PSII, as described above. Rates of cyclic electron transport (CET) around PSI were then estimated by subtracting the measured ETR from the measured rate of electron transport through PSI (Johnson, 2011). CET was measured at intervals over the range of 0–2000 PPFD (from low to high PPFD, 6 min at each irradiance) and CO_2 concentration of 400 µmol mol^{-1}.

A Dual-PAM-100 measuring system equipped with the emitter module DUAL-EP515 and the detector module DUAL-DP515 was used to measure the 550–515 nm absorbance difference signal (Schreiber and Klughammer, 2008). This signal provides a linear measure of thylakoid membrane Δψ due to a Δψ-induced shift in the absorption spectrum of thylakoid pigments, known as the electrochromic shift (ECS). A dark-interval relaxation kinetics (DIRK) analysis of the ECS signal during a light-to-dark transition was used to estimate several parameters related to thylakoid proton flux (Cruz *et al.*, 2005; Baker *et al.*, 2007). These measurements rely upon the principal that, under steady-state conditions, proton influx to the lumen due to electron transport is balanced by proton efflux from the lumen through ATP synthase. As previously described, the total rapid decay in the ECS signal over the initial approximately 300 ms of dark (ECS_t) is an estimate of the total light-induced pmf (Cruz *et al.*, 2005; Baker *et al.*, 2007). A firstorder fit of this rapid exponential decay provides a time constant (τ_{ECS}) inversely proportional to the proton conductivity of ATP synthase (g_H+) calculated as $g_H+=1/\tau_{ECS}$. The relative rate of proton flux across the thylakoid membrane (v_H+) is then estimated as ECS_t/τ_{ECS} (Cruz *et al.*, 2005; Baker *et al.*, 2007). Beyond 300 ms and up to approximately 120 s after the light–dark transition, an inverse ECS signal develops due to continued proton efflux. This signal is exploited to partition ECS_t into two components, ECS_{inv} and ECS_{ss}, corresponding respectively to the ΔpH and Δψ components of the total light-induced pmf, as outlined previously (Cruz *et al.*, 2005; Baker *et al.*, 2007). For the DIRK analysis, plants were dark-adapted for 1 h, followed by illumination (700 or 1600 PPFD) for 10 min prior to the light–dark transition. It should be noted that the ECS signal and its meaning remain controversial due to the possibility of confounding overlapping absorbance signals (Johnson and Ruban, 2014).

Biochemical, growth, and other analyses

Leaf protein amounts were estimated by immunoblot analyses. Protein extraction, protein separation by SDS-PAGE, transfer of proteins to nitrocellulose, and incubation with antibodies were performed as before (Dahal *et al.*, 2014). Primary antibodies (Agrisera, Vännäs, Sweden) were diluted 1000–5000-fold, and raised against the following proteins: PsbA (D1 reaction center protein of PSII), PsbS (a PSII-associated sensor of lumen pH necessary for NPQ induction), PsaA (a reaction center protein of PSI), Cyt_f (the *c*-type cyt subunit of the Cyt b_6f complex), AtpB (the B-subunit of the F_1 catalytic subcomplex of ATP synthase), RbcS (small subunit of Rubisco) and AOX. Secondary antibody was detected by chemiluminescence (Clarity Western ECL Substrate, Bio-Rad Laboratories, Mississauga, Canada) and X-ray film. The signals were quantified using an image analysis system (Chemidoc XRS+ with Image Lab Software v.3.0, Bio-Rad).

To evaluate growth, the dry weight (DW) of different plant parts was determined following oven drying (48 h, 80 °C). Leaf area was

measured with an area meter (Model LI-3000C, LiCor Biosciences, Lincoln, NE, USA). Plant height was measured from stem base to shoot apex. In most cases, growth was analysed at days 23, 33, 39, and 45 of the experiments described above. However, in some cases, the moderate water deficit was extended until day 92, by which time the plants had fully senesced and all seed pots had fully dried. These plants were used to determine seed pod number and weight, and the seed was tested using a germination assay. Germination was tested on agar plates (containing Murashige and Skoog salts, vitamins and 1% sucrose) incubated under constant conditions (75 PPFD, 25 °C) for 7 d.

Total leaf Chl and protein amounts were determined as previously described (Dahal *et al.*, 2014). Leaf RWC was determined as before (Wang and Vanlerberghe, 2013) and also used to determine specific leaf weight. Soil water content (% saturation) at different times during an experiment was determined by measuring the pot weight and comparing it to the pot weight at the beginning of the experiment, when the soil was at field capacity and defined as 100% saturated. Statistical analyses (two-way or one-way ANOVA, followed by a Bonferroni post-test to compare all plant lines within a treatment) were performed using Prism 5.0 (GraphPad Software).

Results

AOX is an important determinant of R_L *during a prolonged water deficit*

On all days, there were no differences in leaf 5 RWC across plant lines, indicating that the differences in the AOX amount across lines had no impact on leaf water status (see Supplementary Fig. S2C). There was a moderate decline in leaf RWC in all lines over the course of the experiment. For example, RWC in the WT was 82% on day 23, 71% on day 33, 67% of day 39 and 70% on day 45. This allowed us to compare the plants under both mild (day 23) and moderate (days 33–45) water deficit conditions, while also maintaining a relatively constant moderate water deficit over an extended period. This allowed us to reveal differences in long-term processes such as growth across the plant lines (see below).

There were gradual changes in several other leaf 5 parameters over the course of the experiment. In WT plants, the mean value of total Chl and total protein declined 24% and 26%, respectively, while the Chl *a*/*b* ratio and specific leaf weight increased 16% and 37%, respectively, between days 23 and 45 (see Supplementary Fig. S3A, C, D). On day 23, these parameters were similar among WT, AOX knockdown, and AOX overexpression plants. However, by day 45, a pattern emerged whereby total Chl and total protein were modestly higher (by 12% and 11%, respectively) in the overexpressors (average of two lines) and modestly lower (by 16% and 15%, respectively) in the knockdowns, compared with WT. By day 45, the mean Chl *a*/*b* ratio was 9% lower in the overexpressors and 18% higher in the knockdowns, compared with WT (Supplementary Fig. S3B). However, there was no difference in leaf 5 specific weight (Supplementary Fig. S3D) or size (Supplementary Fig. S4) across plant lines over the course of the experiment.

There were no significant differences in leaf 5 R_D across plant lines on any of the days examined (Fig. 1A). In all plant lines, there was perhaps a small decline in R_D between day 23 and 33, followed by a recovery of the rate through days 39 and 45. There were also no differences in R_L across plant lines on day 23 (Fig. 1B). However, by day 33, a pattern emerged where R_L was highest in the AOX overexpressors and lowest in the AOX knockdowns, with WT showing an intermediate rate. These differences in R_L were exaggerated further by day 39 and again by day 45. On day 45, the overexpression lines averaged 25% higher R_L and the knockdowns averaged 34% lower R_L than in WT (Fig. 1B).

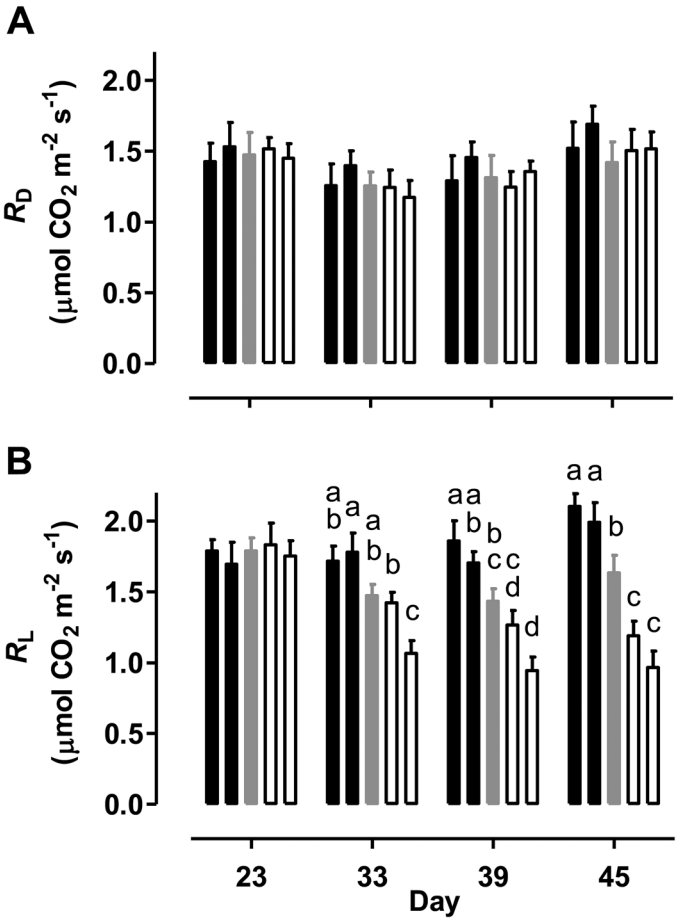

Fig. 1. Respiration rate of tobacco leaf at different times during a prolonged water deficit. (A) R_D. (B) R_L. Data are shown for WT (gray bar), AOX overexpressors (B8, left closed bar; B7, right closed bar), and AOX knockdowns (RI9, left open bar; RI29, right open bar). Data are the mean±SE of three independent experiments (n=3). Within each data set, plant lines not sharing a common letter are significantly different from one another (P<0.05). In data sets without letters, there are no significant differences across plant lines.

AOX respiration improves A *during a prolonged water deficit*

In WT plants, the mean A of leaf 5, measured at growth irradiance, declined from 11.7 to 7.4 µmol CO_2 m^{-2} s^{-1} between days 23 and 33 (Fig. 2A). A further small decline occurred by day 39 (to 6.4 µmol m^{-2} s^{-1}) and then again by day 45 (to 5.3 µmol m^{-2} s^{-1}). Under mild water deficit (day 23), the five plant lines maintained similar mean A. However, by day 33 a pattern emerged where A was slightly higher in the overexpressors and slightly lower in the knockdowns, compared with WT. This pattern was exaggerated further by day 39 and

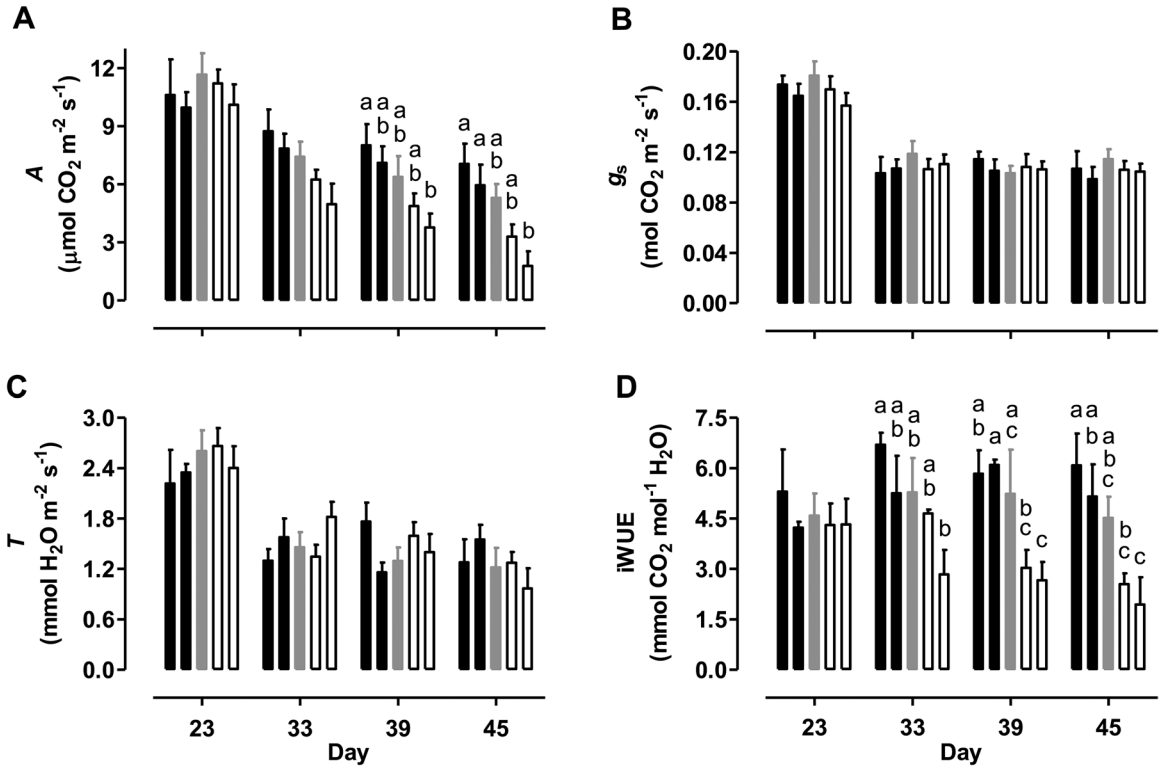

Fig. 2. Photosynthesis-related parameters of tobacco leaf at different times during a prolonged water deficit and measured at the growth irradiance. (A) *A*. (B) g_s. (C) *T*. (D) iWUE. Data are shown for WT (gray bars), AOX overexpressors (B8, left closed bar; B7, right closed bar), and AOX knockdowns (RI9, left open bar; RI29, right open bar). Data are the mean±SE of three independent experiments (n=3). Within each data set, plant lines not sharing a common letter are significantly different from one another (P<0.05). In data sets without letters, there are no significant differences across plant lines.

again by day 45 (Fig. 2A). On day 45, the overexpressors averaged 23% higher *A*, and the knockdowns averaged 52% lower *A* than WT, when measured at the growth irradiance. Light response curves showed similar dramatic differences in *A* across the plant lines over time (see Supplementary Fig. S5).

Leaf 5 g_s and *T* measured at growth irradiance did not differ across plant lines on any of the days examined (Fig. 2B, C). In all lines, these two parameters declined noticeably between days 23 and 33, and then remained relatively constant for the remainder of the experiment. In WT plants, the mean iWUE of leaf 5 measured at growth irradiance was relatively stable (ranging from 4.5 to 5.3 mmol CO_2 mol^{-1} H_2O) throughout the experiment (Fig. 2D). On day 23, iWUE was similar across all plant lines. However, at the later days (particularly days 39 and 45), mean iWUE was highest in the overexpressors and lowest in the knockdowns, with WT showing an intermediate value. On day 45, mean iWUE was 25% higher in the overexpressors and 50% lower in the knockdowns, compared with WT (Fig. 2D).

Leaf 5 Chl *a* fluorescence analyses indicated that all plant lines exhibited similar ETR, NPQ and PSII excitation pressure (1−qP) on day 23, over a wide range of irradiance (see Supplementary Figs S6–S8). At later days, however, the overexpressors maintained higher ETR and lower NPQ and 1−qP than WT while the knockdowns maintained lower ETR and higher NPQ and 1−qP than WT, particularly at higher irradiance (Supplementary Figs S6–S8).

Figure 3 shows the relationship between NPQ and ETR. It indicates that, over the course of the experiment, the plants were able to generate a higher NPQ despite having a lower ETR. Further, this increased 'sensitivity' of NPQ to ETR was clearly enhanced in the knockdowns and reduced in the overexpressors, relative to WT, during the moderate water deficit period (days 33–45) (Fig. 3).

Absorption spectroscopy combined with a DIRK analysis was used to both quantify leaf 5 pmf and partition the pmf into its Δψ and ΔpH components. On day 23, ECS_t, a measure of pmf, did not differ across plant lines when measured at growth irradiance (Fig. 4A). However, by day 33, a pattern emerged where the overexpressors maintained a lower and the knockdowns maintained a higher ECS_t than WT. This pattern became more pronounced by day 39 and again by day 45. On day 45, ECS_t averaged 23% lower in the overexpressors and 30% higher in the knockdowns than in WT. These differences were not due to differences in the Δψ component of the pmf, measured as ECS_{ss}, which remained similar across plant lines throughout the experiment (Fig. 4B). Instead, ΔpH (measured as ECS_{inv}) differed across lines on days 33–45. For example, on day 45, mean ECS_{inv} was 26% lower in the overexpressors and 44% higher in the knockdowns, compared with WT (Fig. 4C). The percentage contribution of ΔpH toward the total pmf did not differ across plant lines (Fig. 4D).

The DIRK analysis was also used to quantify the rate of proton flux from stroma to lumen (v_H+) and the conductance of the thylakoid membrane to proton movement from lumen to stroma (g_H+) at the growth irradiance. In the WT, v_H+ was relatively stable over the course of the experiment (Fig. 5A), while g_H+ declined noticeably (by 22%) between day 23

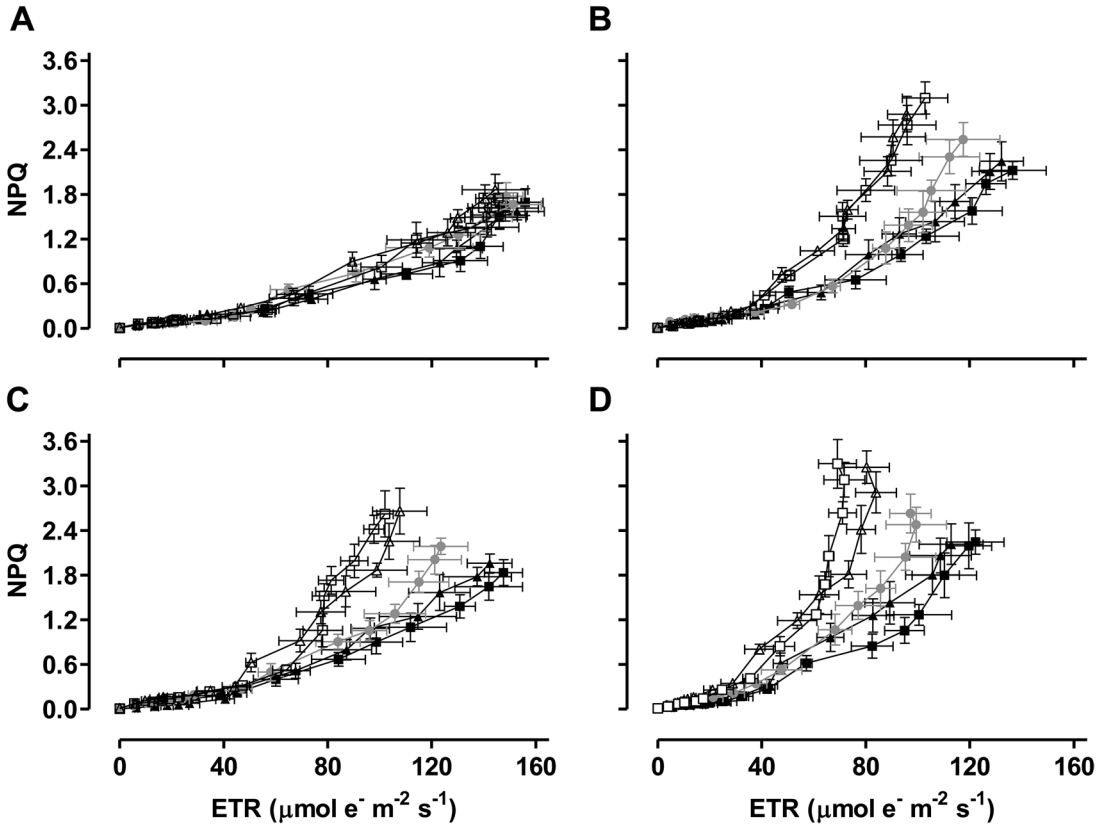

Fig. 3. The relationship between ETR and NPQ at different times during a prolonged water deficit and measured at the growth irradiance. (A) Day 23. (B) Day 33. (C) Day 39. (D) Day 45. Data are the mean±SE of three independent experiments (n=3). Data are presented for WT (gray circle), AOX overexpressors (B7, closed triangle; B8, closed square), and AOX knockdowns (RI9, open triangle; RI29, open square). ETR and NPQ data for each individual line and over a wide range of measurement irradiances is presented in Supplementary Figs S6 and S7.

and 33, and was then maintained at this lower conductance through day 45 (Fig. 5B). The v_H+ did not differ across plant lines on any of the days examined (Fig. 5A). On day 23, g_H+ was also similar across plant lines. However, by day 33, a pattern emerged where the overexpressors maintained higher g_H+ and the knockdowns maintained lower g_H+ than WT. This pattern became more pronounced through days 39 and 45. On day 45, the mean g_H+ was 23% higher in the overexpressors and 34% lower in the knockdowns than in WT (Fig. 5B). All of the above DIRK analyses were also performed at a saturating irradiance and yielded similar findings to those described above (Supplementary Figs S9 and S10).

Combined Chl fluorescence and PSI absorption spectroscopy analyses indicated that all plant lines exhibited similar rates of leaf 5 CET, measured at growth irradiance, on day 23 (Fig. 5C). At later days, however, the overexpressors maintained lower rates and the knockdowns maintained higher rates of CET than the WT. Supplementary Fig. S11 shows rates of CET of each plant line across a wide range of measurement irradiances.

Immunoblot analyses compared the amount of AOX and several key photosynthetic proteins in leaf 5 across the plant lines. For these analyses, equal amounts of protein extract from RI9 and RI29 or B7 and B8 were combined prior to analysis. In WT, AOX protein amount increased strongly in response to moderate water deficit. Compared with day 23, AOX amount was increased 4.5-, 5.6-, and 5.9-fold on days 33, 39, and 45, respectively (Fig. 6A). This increase in AOX protein amount correlated with an increase in the excitation pressure being experienced by these plants (see Supplementary Fig. S12). We have reported before that growth excitation pressure appears an important factor influencing AOX amount across various growth conditions (Dahal *et al.*, 2017). As expected, AOX protein amount was always higher in the overexpressors and lower in the knockdowns, compared with WT. On day 23, AOX amount in overexpressors was 9.1-fold higher than WT, while AOX amount in knockdowns was only 17% of the WT amount. During moderate water deficit, AOX amount remained 2-fold higher in overexpressors than WT, while AOX amount in knockdowns was only 14% of the WT amount (average of days 33, 39, and 45) (Fig. 6A).

Of the six different photosynthetic proteins examined, none differed in amount between WT, overexpressors, and knockdowns during mild water deficit (day 23) (Figs 5D and 6). However, the amount of some proteins did differ dramatically across plant lines during the moderate water deficit period. In WT, the protein amount of AtpB (the B-subunit of the F_1 catalytic subcomplex of ATP synthase) was 28% lower during moderate water deficit (average of days 33, 39, and 45) compared with mild water deficit (Fig. 5D). However, this decline was less severe in the overexpressors and more severe in the knockdowns. Hence, the AtpB protein amount during moderate water deficit (average of days 33, 39, and

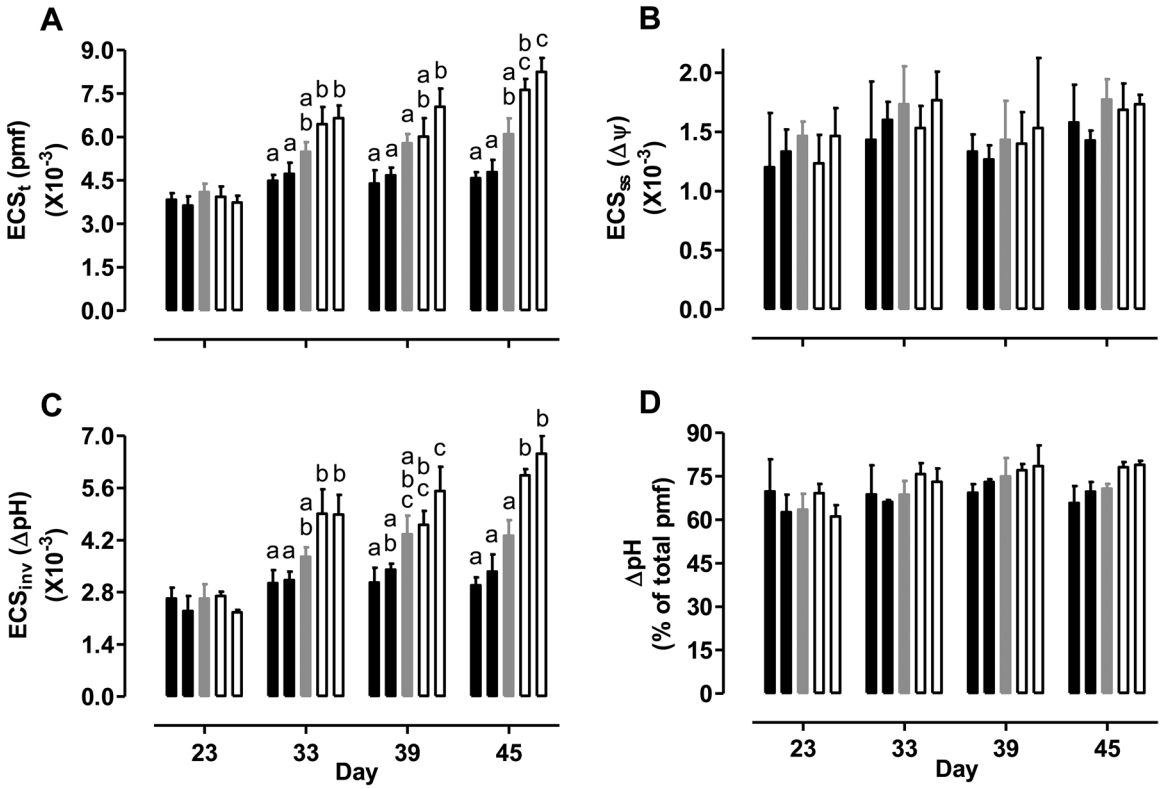

Fig. 4. Thylakoid membrane pmf and the partitioning of pmf into its Δψ and ΔpH components in tobacco leaf at different times during a prolonged water deficit, and measured at the growth irradiance. (A) ECS_t, a measure of pmf. (B) ECS_{ss}, a measure of Δψ. (C) ECS_{inv}, a measure of ΔpH. (D) ΔpH as a percentage of the total pmf. Data are shown for WT (gray bars), AOX overexpressors (B8, left closed bar; B7, right closed bar), and AOX knockdowns (RI9, left open bar; RI29, right open bar). Data are the mean±SE of three independent experiments (n=3). Within each data set, plant lines not sharing a common letter are significantly different from one another (P<0.05). In data sets without letters, there are no significant differences across plant lines.

45) was 19% higher in the overexpressors and 31% lower in the knockdowns, compared with WT (Fig. 5D).

The protein amount of PsbA (D1 reaction center protein of PSII) was unchanged over the course of the experiment and did not differ across plant lines (Fig. 6B). However, PsaA (a reaction center protein of PSI) increased in response to moderate drought. Compared with day 23, PsaA amount in the WT was increased 1.3-, 1.4-, and 1.6-fold on days 33, 39, and 45, respectively. Further, this increase was exaggerated in the knockdowns but less evident in the overexpressors. Hence, the PsaA amount during moderate water deficit (average of days 33, 39, and 45) was 38% higher in the knockdowns and 25% lower in the overexpressors, compared with WT (Fig. 6C). Cyt_f (the c-type cyt subunit of the Cyt b_6f complex) amount was more variable over the course of the experiment, but was lower during moderate than mild water deficit. However, the dynamic changes in Cyt_f amount were always similar across plant lines (Fig. 6D). In the WT, PsbS (a PSII-associated sensor of lumen pH necessary for NPQ induction) amount increased in response to moderate water deficit. Compared with day 23, PsbS amount was increased 1.6-, 1.7-, and 1.8-fold on days 33, 39, and 45, respectively. This increase was enhanced in the knockdowns, but less evident in the overexpressors. Hence, the PsbS amount during moderate water deficit (average of days 33, 39, and 45) was 45% higher in the knockdowns and 29% lower in the overexpressors, compared with WT (Fig. 6E). Compared with mild water deficit (day 23), RbcS (small subunit of Rubisco) amount in the WT declined by 40% during the moderate water deficit period (average of days 33, 39, and 45). This decline was more severe in the knockdowns and less severe in the overexpressors. Hence, the RbcS amount during moderate water deficit (average of days 33, 39, and 45) was 40% lower in the knockdowns and 37% higher in the overexpressors, compared with WT (Fig. 6F). For all of the immunoblot analyses described above, representative Western blots are shown in Supplementary Fig. S13.

AOX respiration improves growth during a prolonged water deficit

On day 23, all plant lines displayed similar leaf, stem and total above-ground biomass, measured as DW (Fig. 7). However, by day 45, total above-ground biomass averaged 19% higher in the AOX overexpressors and 18% lower in the AOX knockdowns, compared with WT (Fig. 7D). This difference across plant lines was primarily due to differences in the biomass of stem tissue and reproductive tissue (flowers and seed pods) (Fig. 7B, C). In these tissues, the biomass trends across plant lines mirrored the trends seen in leaf 5 A rates across the plant lines during the moderate water deficit period.

Reproductive tissue as a percentage of total above-ground biomass declined with declining AOX amount. On day 45, reproductive tissue averaged 24.5% of total biomass in the

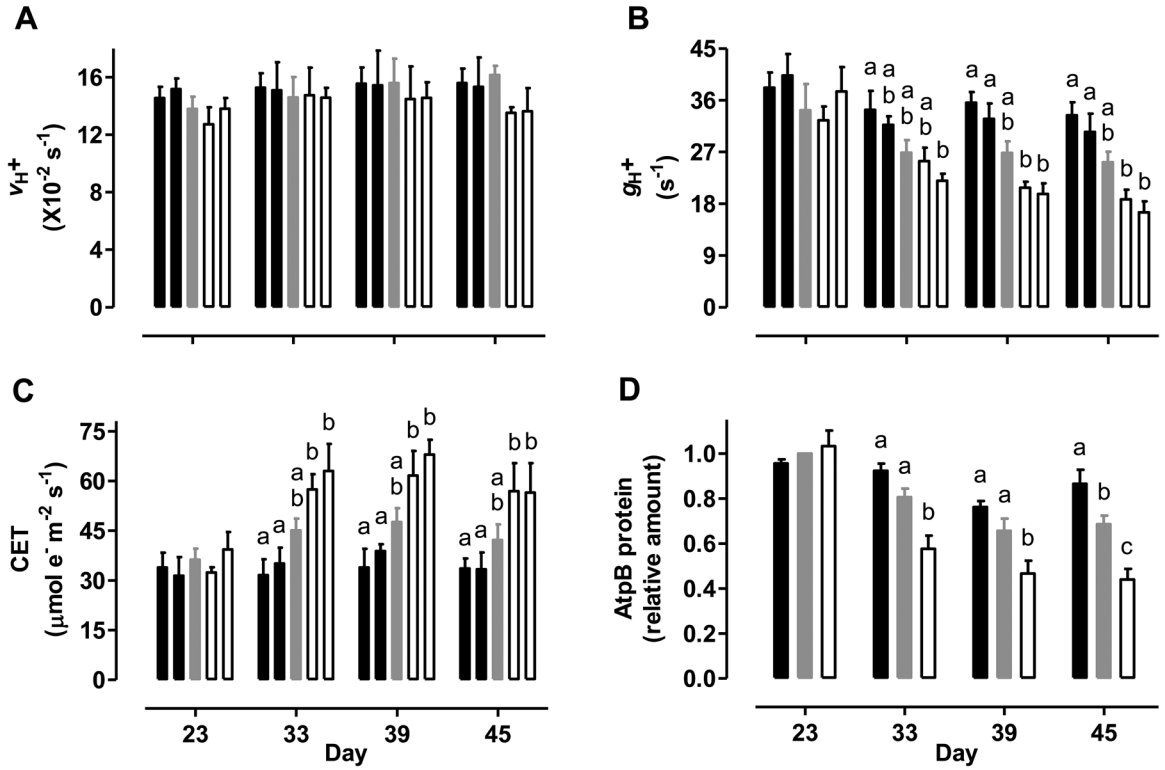

Fig. 5. Thylakoid membrane proton flux-related parameters in tobacco leaf at different times during a prolonged water deficit. (A) The rate of proton flux from stroma to lumen. (B) The conductance of the thylakoid membrane for proton movement from lumen to stroma. (C) The rate of CET around PSI. (D) The amount of leaf AtpB protein. The measurements in (A–C) were made at the growth irradiance. In (A–C) data are presented for WT (gray bar), AOX overexpressors (B8, left closed bar; B7, right closed bar), and AOX knockdowns (RI9, left open bar; RI29, right open bar). In (D), data are presented for WT (gray bar), combined B8 and B7 (closed bar), and combined RI9 and RI29 (open bar). The AtpB protein amounts are relative to the amount in the WT on day 23, which was set to 1. All data are the mean±SE of three independent experiments (n=3). Within each data set, plant lines not sharing a common letter are significantly different from one another (P<0.05). In data sets without letters, there are no significant differences across plant lines.

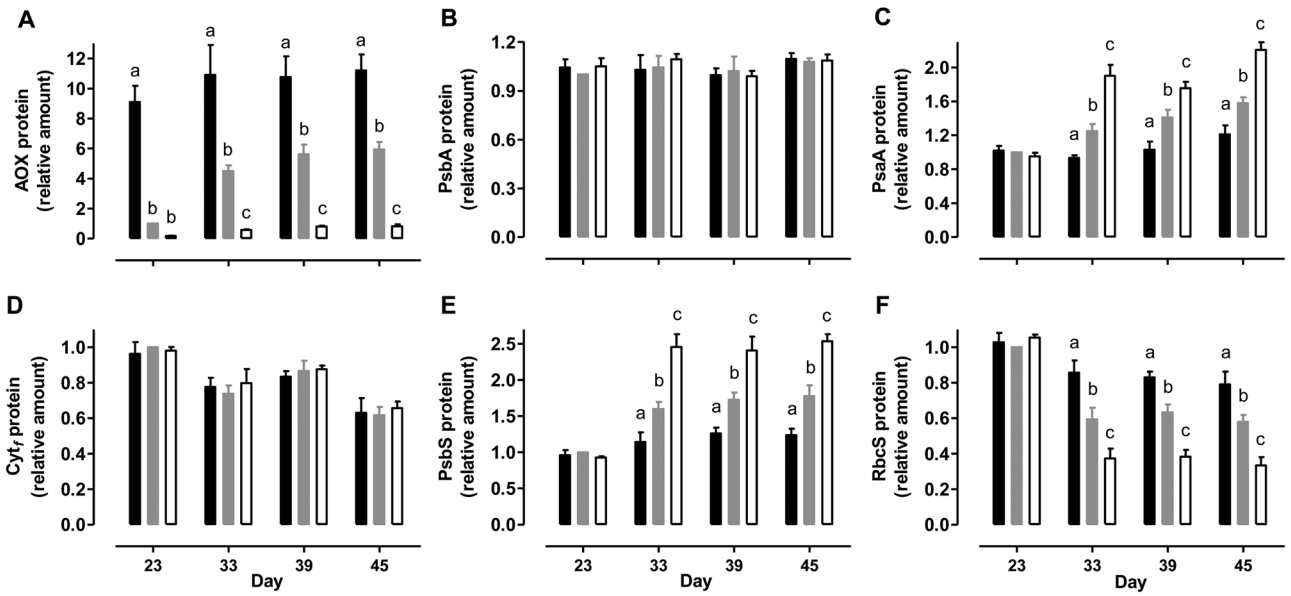

Fig. 6. Amounts of AOX and different photosynthesis-related proteins in tobacco leaf at different times during a prolonged water deficit. (A) AOX. (B) PsbA. (C) PsaA. (D) Cyt$_f$. (E) PsbS. (F) RbcS. Data are presented for WT (gray bar), combined B8 and B7 (closed bar), and combined RI9 and RI29 (open bar). Protein amounts are relative to the amount in the WT on day 23, which was set to 1. Data are the mean±SE of three independent experiments (n=3). Within each data set, plant lines not sharing a common letter are significantly different from one another (P<0.05). In data sets without letters, there are no significant differences across plant lines.

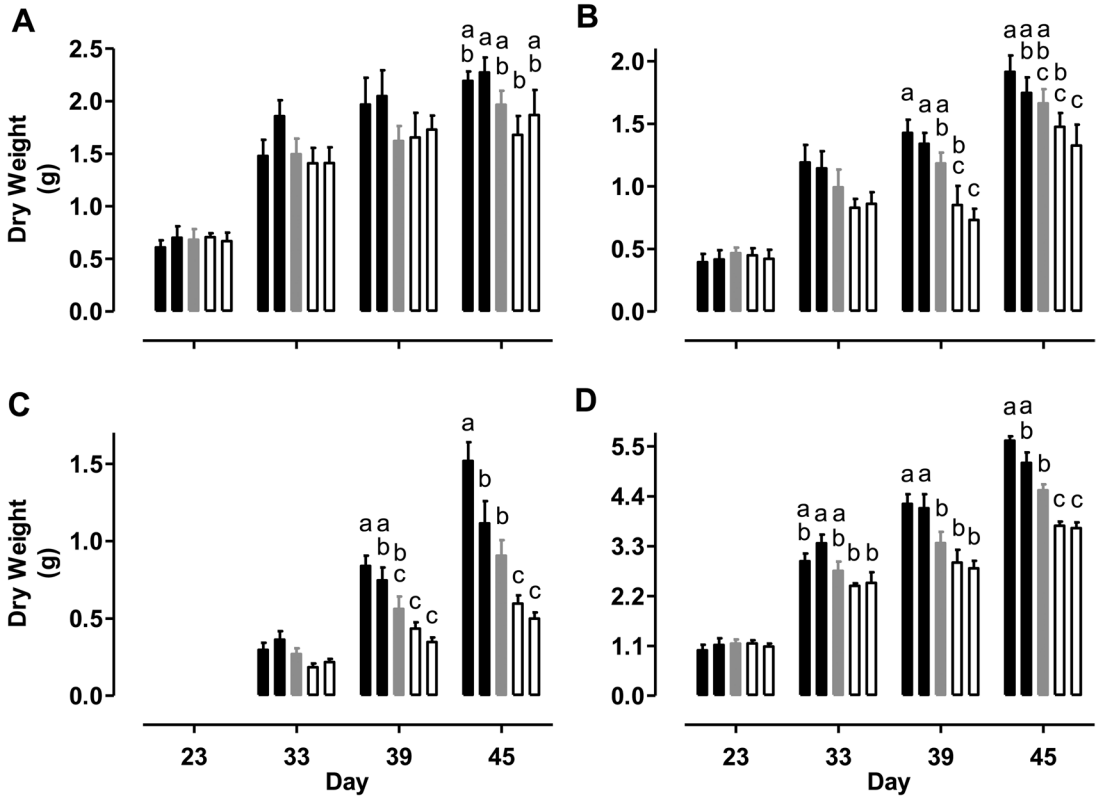

Fig. 7. Tobacco plant DW at different times during a prolonged water deficit. Data are shown for (A) leaves, (B) stem, (C) reproductive tissue (flowers, seed pods) and (D) total shoot [sum of (A–C)]. Data are presented for WT (gray bar), AOX overexpressors (B8, left closed bar; B7, right closed bar), and AOX knockdowns (RI9, left open bar; RI29, right open bar). Data are the mean±SE of three independent experiments (n=3). Within each data set, plant lines not sharing a common letter are significantly different from one another (P<0.05). In data sets without letters, there are no significant differences across plant lines.

overexpressors, 20% of total biomass in the WT, and just 15% of total biomass in the knockdowns. On the other hand, total leaf biomass by day 45 (and on the other days) was more variable across plant lines, although there was still some tendency for elevated leaf biomass in the overexpressors (13% higher mean value than WT on day 45) and reduced leaf biomass in the knockdowns (10% lower mean value than WT on day 45) (Fig. 7A). There were also no clear differences in total leaf area across the plant lines on any days (see Supplementary Fig. S14). A separate set of experiments only evaluated plant DW (leaf, stem, and reproductive tissue) at day 45 and yielded similar results to all those described above (Supplementary Fig. S15). In this case, total above-ground biomass averaged 17% higher in the overexpressors and 27% lower in the knockdowns than in WT.

Measurements of plant height indicated an earlier stem bolting in overexpressors and a delayed stem bolting in knockdowns, compared with WT (Fig. 8A). Further, the appearance of first flowers occurred 3–4 days earlier in the overexpressors and 5–8 days later in the knockdowns, compared with WT (Fig. 8B). Interestingly, though, plant height at the time of emergence of the first flowers (large data points in Fig. 8A) remained similar across the plant lines.

A separate set of experiments extended the moderate water deficit beyond day 45, to day 92. At day 92, the mean final number of seed pods per plant was 23% higher in the overexpressors and 24% lower in the knockdowns than in WT (Fig. 8C). Further, total seed pod weight was 38% higher in the overexpressors and 52% lower in the knockdowns than in WT (Fig. 8C). A germination test indicated that, regardless of plant line, the seed being generated was viable (i.e. >90% germination rate).

Discussion

The metabolism and growth of WT tobacco were compared with those of AOX knockdown (RI9, RI29) and overexpression (B7, B8) lines. The comparison was of plants that had experienced a mild to moderate water deficit since the seedling stage, which will have allowed them to acclimate to the limited water availability (Harb *et al.*, 2010; Hummel *et al.*, 2010; Baerenfaller *et al.*, 2012; Schöttler and Tóth, 2014; Avramova *et al.*, 2015; Clauw *et al.*, 2015; Bechtold *et al.*, 2016). A high AOX amount (overexpression lines) increased both photosynthesis and growth, while a low AOX amount (knockdown lines) compromised photosynthesis and growth, relative to WT plants with intermediate amounts of AOX. The differences in photosynthesis and growth across plant lines were not due to differences in leaf water relations or leaf expansion, both of which are key parameters to consider when examining plant performance, particularly under water deficit (Lawlor, 2013; Weraduwage *et al.*, 2015). For example, there were no obvious AOX-dependent differences across the plant lines in leaf RWC, g_s, T, total leaf area, leaf size, total

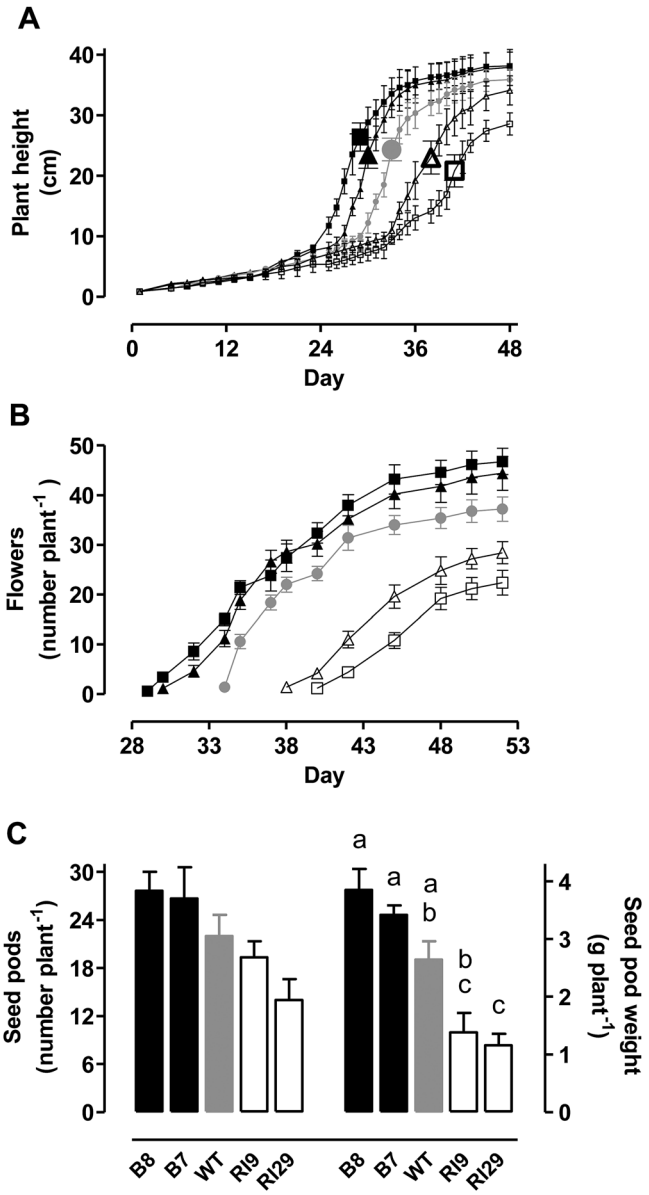

Fig. 8. Tobacco growth and development during a prolonged water deficit. (A) Plant height over time. (B) Total number of flowers emerged over time. (C) Total number of seed pods (left axis and data set) and total DW of seed pods (right axis and data set). In (A, B) data are presented for WT (gray circle), AOX overexpressors (B7, closed triangle, B8, closed square), and AOX knockdowns (RI9, open triangle; RI29, open square), and are the mean±SE of three to five independent experiments (n=3–5). The large symbols in (A) denote the day when first flower(s) appeared. In (C) the data were collected following a water deficit experiment extended until day 92, when all plants were completely senesced and dry; and data are the mean±SE of three independent experiments (n=3). Within each data set, plant lines not sharing a common letter are significantly different from one another (P<0.05). In data sets without letters, there are no significant differences across plant lines.

leaf DW, or specific leaf weight on any of the days examined. Instead, AOX amount appeared to primarily influence fundamental biochemical regulatory mechanisms in the chloroplast that are known to control and fine-tune photosynthetic activity in response to metabolic and environmental conditions. In turn, photosynthetic activity strongly influenced growth, particularly of reproductive sinks, despite the water limitation. These are the subjects of the discussion below.

Maintenance of chloroplast energy balance by the mitochondrion is a critical factor preventing a biochemical limitation of photosynthesis induced by water deficit

We previously showed that when tobacco plants, having been grown and developed under well-watered conditions, were subjected to a relatively rapid onset of water deficit, leaf R_L was reprogrammed. There was a strong increase in AOX respiration alongside a strong decline in cyt oxidase capacity (Dahal *et al.*, 2014; Dahal and Vanlerberghe, 2017). Such a shift in the path of electron flow reduces the ATP yield of the mitochondrion, while maintaining its ability to act as an electron sink. Under these rapid-onset, short-term stress conditions, where A and hence ATP and NADPH consumption by the Calvin cycle were being strongly curtailed, this shift in mitochondrial metabolism supported chloroplast energy balance (Dahal and Vanlerberghe, 2017). The current study extends previous findings by showing that, even in plants where long-term growth and development has occurred under steady-state moderate water deficit conditions, the mitochondrion remains an essential player in supporting chloroplast energy balance. For example, excitation pressure, the fraction of closed (reduced) PSII reaction centers, was increased in the AOX knockdowns and reduced in the AOX overexpressors, compared with WT. This was evident despite long-term adjustments of the photosynthetic apparatus across plant lines that should counteract the excitation pressure differences. In particular, PSI content (measured as PsaA protein amount) was increased in the knockdowns and reduced in the overexpressors, compared with WT. All else being equal, this adjustment should alleviate excitation pressure in the knockdowns and elevate excitation pressure in the overexpressors, relative to WT. As discussed below, this impact of AOX on chloroplast energy balance during water deficit had significant effects on the paths of proton and electron flow (i.e. the proton circuit) in the thylakoid membrane, which then had important consequences for overall photosynthetic activity.

LET (or ETR) is coupled to proton influx from stroma to lumen. An important regulatory function of the resulting low lumen pH is the activation of NPQ, a key means to balance the synthesis of ATP and NADPH by the thylakoid reactions with the consumption of these intermediates by downstream metabolism, particularly the Calvin cycle (Foyer *et al.*, 2012; Tikhonov, 2013). Here, acclimation of WT tobacco to moderate water deficit was associated with a higher NPQ at any given ETR, as was also seen in wild watermelon (Kohzuma *et al.*, 2009). Such changes in the 'sensitivity' of NPQ to ETR is an important regulatory phenomenon since conditions that typically require a high NPQ, such as restrictions in downstream metabolism, are also conditions that will typically suppress ETR and the associated proton influx necessary to activate NPQ (Cruz *et al*, 2005; Armbruster *et al*, 2017). Avenson et al. (2004, 2005) emphasized four major mechanisms by which the sensitivity of NPQ to ETR might be increased. (i) While the H^+/e^- ratio of LET is fixed, the overall H^+/e^- ratio could be increased using CET. This supports further proton influx, and hence NPQ generation, without changing the rate of LET. (ii) Since the extent of the proton

gradient established by LET also depends upon proton efflux from lumen to stroma, a decrease in the proton conductance of chloroplast ATP synthase is another potential means to enhance the sensitivity of NPQ to ETR. (iii) Since NPQ generation requires key protonation events, a change in the partitioning of the pmf away from Δψ and toward ΔpH could enhance the NPQ achieved by a given pmf. Changes in partitioning depend upon changes in the transport of counterions (Cruz *et al.*, 2001; Armbruster *et al.*, 2014; Herdean *et al.*, 2016). (iv) An increase in the capacity of components being controlled by protonation, such as PsbS or violaxanthin deepoxidase, could enhance NPQ at a given proton concentration (Avenson *et al.*, 2004, 2005).

Interestingly, the increased sensitivity of NPQ to ETR during moderate water deficit was greater in the AOX knockdowns and less in the AOX overexpressors, compared with the WT response. This altered sensitivity across plant lines appeared to involve at least some of the mechanisms listed above. First, measured rates of CET were higher in the knockdowns and lower in the overexpressors, compared with WT. In fact, these differences in CET across plant lines may be underestimated since they depend upon the assumption that the partitioning of light energy absorption between PSII and PSI does not differ across the plant lines (Johnson, 2011). However, as discussed earlier, we found evidence that the PSI amount, but not the PSII amount, differed across the plant lines in response to moderate water deficit. Knockdowns had a higher amount of PsaA protein and overexpressors had a lower amount of PsaA protein than WT. If these differences across plant lines translate into similar differences in the partitioning of light energy absorption between the photosystems, then the actual differences in CET across lines will be greater than reported here. Regardless of actual rates, the qualitative differences in CET across plant lines provides an explanation of why rates of v_H+, which is a measure of total proton influx regardless of it being supported by LET or CET, did not differ appreciably across the plant lines despite their differing ETR. The knockdowns are compensating for their lower ETR and associated proton influx, relative to WT, by increasing CET and its associated proton influx. Similarly, the overexpressors are compensating for their higher ETR by displaying lower rates of CET (Shikanai and Yamamoto, 2017).

Besides modulating CET, the difference in sensitivity of NPQ to ETR across plant lines was also achieved by manipulating proton efflux from lumen to stroma. The ECS analyses showed that, while moderate water deficit reduced g_H+ in all plant lines compared with the mild water deficit condition, this reduction was most severe in the knockdowns and least severe in the overexpressors, with WT showing an intermediate response. Changes in g_H+ can be achieved through long-term coarse control of ATP synthase protein amount and/or short-term fine biochemical control of ATP synthase activity (Kanazawa and Kramer, 2002; Kiirats *et al.*, 2009; Yamori *et al.*, 2011*b*; Schöttler *et al.*, 2015; Carrillo *et al.*, 2016; Kohzuma *et al.*, 2017; Schmidt *et al.*, 2017). Here, WT tobacco responded to a prolonged moderate water deficit by reducing ATP synthase amount (estimated by AtpB protein amount) by 19–34%, depending on the day. The measured g_H+ declined by a similar amount (22–27%), suggesting that coarse control of ATP synthase protein amount could largely explain the change in g_H+. A similar conclusion can be drawn for the transgenic lines. In the knockdowns during moderate water deficit (average of three days and two lines), g_H+ and AtpB were 41% and 52% lower, respectively, than under mild water deficit. On the other hand, g_H+ and AtpB in the overexpressors during moderate water deficit were 16% and 11% lower, respectively, than under mild water deficit.

A change in the partitioning of the pmf away from Δψ and toward ΔpH could be another means to enhance NPQ at a given ETR. Here, ΔpH as a percentage of the total pmf increased slightly over the course of the experiment in all plant lines. Also, the knockdowns tended to display a slightly higher partitioning toward ΔpH, and the overexpressors tended to display a slightly lower partitioning toward ΔpH, compared with WT, during moderate water deficit. However, these differences were relatively minor compared with the differences in CET and ATP synthase amount described above. A larger difference was seen in the protein amount of PsbS across plant lines. Hence, it could also be contributing toward the differences in sensitivity of NPQ to ETR across the plant lines.

A consensus has developed that declines in photosynthesis during water deficit can be the result of biochemical limitation(s) that reduce A over and above that due to stomatal closure and the ensuing CO_2 limitation (Lawlor, 2002; Flexas *et al.*, 2004; Grassi and Magnani, 2005; Lawlor and Tezara, 2009; Rivero *et al.*, 2009; Pinheiro and Chaves, 2011; Perez-Martin *et al.*, 2014; Zhou *et al.*, 2014). In several species, this biochemical limitation has been linked to ATP synthase amount and activity, suggesting this to be a widespread phenomenon (Tezara *et al.*, 1999; Kohzuma *et al.*, 2009; Hoshiyasu *et al.*, 2013; Dahal *et al.*, 2014). Modulation of ATP synthase acts to define the upper limit of ETR (and hence A) that is possible before becoming constrained by rising NPQ, as well as increased photosynthetic control at the cyt b_6f complex (Rott *et al.*, 2011; Foyer *et al.*, 2012; Tikhonov, 2014). Based on the current study, it is clear that AOX respiration impacts chloroplast energy balance during water deficit, disrupting the thylakoid proton circuit, and hence influencing the onset of this biochemical limitation of photosynthesis.

Given the above discussion, a critical question is, what is the signal(s) controlling ATP synthase amount? In other words, what metabolic conditions under water deficit are triggering the ATP synthase decline? This decline was less severe in AOX overexpressors and more severe in AOX knockdowns, compared with WT, which might provide a clue(s) to the metabolic conditions responsible. Under water deficit, AOX amount is a strong determinant of R_L, which in turn correlates strongly with excitation pressure (Dahal and Vanlerberghe, 2017; Dahal *et al.*, 2017). When AOX is lower, R_L is lower and excitation pressure is higher. This is strong evidence that consumption of electrons by AOX is important in preventing an over-reduction of the photosynthetic electron transport chain during water deficit. Such over-reduction, or some consequence of this over-reduction

(e.g. oxidative damage or ROS signaling; Mahler *et al.*, 2007, Lawlor and Tezara, 2009; Noctor *et al.*, 2014; Foyer *et al.*, 2017) might be the condition responsible for down-regulation of ATP synthase amount. While the cyt pathway can also consume electrons, a concerted shift away from this path and toward AOX will lower the mitochondrial ATP yield per electron consumed. This might allow increased activity of additional chloroplast electron sinks (e.g. Mehler reaction) otherwise restricted by rates of ATP turnover (Dahal *et al.*, 2015). Hence, some component of adenylate energy status, such as ATP or P_i amount is another potential underlying factor that could be controlling ATP synthase amount (Shikanai and Yamamoto, 2017).

Previous studies have noted that water deficit-induced biochemical limitations of photosynthesis can coincide with declines in Rubisco amount or activity (Tezara *et al.*, 2002; Dahal *et al.*, 2014). Here, the changes in AtpB and RbcS amount were remarkably similar, suggesting that their amounts are being tightly coordinated. This is perhaps part of a more general system acting to harmonize the capacity of the thylakoid and stromal reactions (Yamori *et al.*, 2010; Schöttler and Tóth, 2014; Yang *et al.*, 2016*a*). Hence, our current hypothesis is that the change in Rubisco amount is a secondary consequence of the change in ATP synthase amount.

Biochemical limitations of photosynthesis can have a significant impact on water use efficiency and growth during water deficit

A potentially powerful approach to improve plant performance under water-limiting conditions is to increase iWUE, the ratio of instantaneous CO_2 uptake to water loss by the leaf during photosynthesis (Araus *et al.*, 2002; Condon *et al.*, 2002, 2004; Polley, 2002; Gago *et al.*, 2014). This could be achieved by decreasing T, increasing A, or by some favorable combination of the two. In biotechnological studies in which leaf iWUE has been shown to differ across plant lines, improved iWUE has almost always been associated with a decrease in T, due, for example, to changes in stomatal density or function (reviewed in Lawlor, 2013). In other studies, the efficiency of whole plant water use has been made more favorable, due, for example, to broader changes in leaf and/or root growth and development (Masle *et al.*, 2005; Karaba *et al.*, 2007; Thompson *et al.*, 2007; Yu *et al.*, 2008; Rivero *et al.*, 2009; Lawlor, 2013; Yang *et al.*, 2016*b*; Hughes *et al.*, 2017). Nonetheless, using the above approaches to increase plant performance and yield has proven challenging since, while they may improve performance during water deficit, they are also often associated with a growth penalty when water is not limiting (Lawlor, 2013). When raised under well-watered conditions or when experiencing only a mild water deficit, the WT, knockdown and overexpression plants used here all display similar A and T under a wide range of growth and measurement irradiances (Dahal *et al.*, 2017). However, the current study indicates that, once a threshold severity of prolonged water deficit is achieved, large differences in iWUE develop across the plant lines, due solely to differences in A. This demonstrates that, through a manipulation in photosynthesis–respiration interactions, it is possible to increase iWUE, photosynthesis and growth under water-limiting conditions, and without any obvious compromising of performance when water is more plentiful (Nunes-Nesi *et al.*, 2011).

One consequence of the growth conditions used in this study was that the plants were still relatively small when they began to flower. This likely represents 'stress-induced flowering', a developmental phenomenon documented in many species and in response to diverse abiotic stresses, including water deficit (Takeno, 2016). Further, there were clear differences in flowering time across the plant lines, with overexpressors flowering earlier and knockdowns flowering later. Interestingly, when Liu *et al.* (2009) compared WT tobacco to transgenic lines with increased or decreased amount of a mitochondrial external NADPH dehydrogenase, they found that differences in plant height and flowering time across the plant lines correlated with differences in the $NADPH/NADP^+$ ratio of specifically the stem tissue. High stem $NADPH/NADP^+$ slowed increases in plant height and delayed flowering time. All plant lines did, however, flower once reaching a similar threshold height, which is similar to the findings here. The differences in flowering time across plant lines in the current study might represent an interesting system to elucidate cue(s) responsible for stress-induced flowering, which are poorly understood (Takeno, 2016).

Most of the final difference in shoot biomass accumulation across plant lines was due to the reproductive sinks (flowers, seeds). This indicates that biotechnological manipulations altering A may preferentially impact on these strong sinks for photosynthate, particularly under 'stress-induced flowering' conditions such as prolonged water deficit. Finally, our results may relate to a study in which AOX overexpression improved the growth of Arabidopsis seedlings exposed to osmotic stress or water deficit (Skirycz *et al.*, 2010). Whether photosynthesis played a role in those growth differences has, to our knowledge, not been reported.

Supplementary data

Supplementary data are available at *JXB* online.

Fig. S1. The irrigation schedule used to compare the metabolism and growth of WT and transgenic tobacco plants during a prolonged water deficit.

Fig. S2. Water status of tobacco leaf at different times during a prolonged water deficit.

Fig. S3. Characteristics of tobacco leaf at different times during a prolonged water deficit.

Fig. S4. Tobacco leaf dimensions at different times during a prolonged water deficit.

Fig. S5. Tobacco leaf A rates as a function of irradiance (light response curves) during a prolonged water deficit.

Fig. S6. Tobacco leaf PSII ETR (LET) as a function of irradiance during a prolonged water deficit.

Fig. S7. Tobacco leaf NPQ as a function of irradiance during a prolonged water deficit.

Fig. S8. Tobacco leaf PSII excitation pressure as a function of irradiance during a prolonged water deficit.

Fig. S9. Thylakoid membrane pmf and the partitioning of pmf into its $\Delta\psi$ and ΔpH components in tobacco leaf at different times during a prolonged water deficit.

Fig. S10. Thylakoid membrane proton flux-related parameters in tobacco leaf at different times during a prolonged water deficit.

Fig. S11. Rates of CET around PSI in tobacco leaf as a function of irradiance and at different times during a prolonged water deficit.

Fig. S12. The relationship between PSII excitation pressure (1−qP) measured at the growth irradiance and leaf AOX protein amount in WT tobacco at different times during a prolonged water deficit.

Fig. S13. Representative immunoblots for AOX and several photosynthesis-related proteins at different times during a prolonged water deficit.

Fig. S14. Total tobacco plant leaf area at different times during a prolonged water deficit.

Fig. S15. Tobacco plant DW after a prolonged water deficit.

Acknowledgements

Financial support was provided by the Natural Sciences and Engineering Research Council of Canada to G.C.V.

Author contributions

KD performed most of the experiments and commented on the writing; KD and GCV designed the experiments and analysed the data; GCV conceived the project and wrote the article.

References

Alber NA, Sivanesan H, Vanlerberghe GC. 2017. The occurrence and control of nitric oxide generation by the plant mitochondrial electron transport chain. Plant, Cell & Environment **40,** 1074–1085.

Amthor JS. 2010. From sunlight to phytomass: on the potential efficiency of converting solar radiation to phyto-energy. New Phytologist **188,** 939–959.

Araus JL, Slafer GA, Reynolds MP, Royo C. 2002. Plant breeding and drought in C_3 cereals: what should we breed for? Annals of Botany **89,** 925–940.

Armbruster U, Carrillo LR, Venema K, *et al*. 2014. Ion antiport accelerates photosynthetic acclimation in fluctuating light environments. Nature Communications **5,** 5439.

Armbruster U, Correa Galvis V, Kunz HH, Strand DD. 2017. The regulation of the chloroplast proton motive force plays a key role for photosynthesis in fluctuating light. Current Opinion in Plant Biology **37,** 56–62.

Avenson TJ, Cruz JA, Kramer DM. 2004. Modulation of energy-dependent quenching of excitons in antennae of higher plants. Proceedings of the National Academy of Sciences, USA **101,** 5530–5535.

Avenson TJ, Cruz JA, Kanazawa A, Kramer DM. 2005. Regulating the proton budget of higher plant photosynthesis. Proceedings of the National Academy of Sciences, USA **102,** 9709–9713.

Avramova V, AbdElgawad H, Zhang Z, *et al*. 2015. Drought induces distinct growth response, protection, and recovery mechanisms in the maize leaf growth zone. Plant Physiology **169,** 1382–1396.

Baerenfaller K, Massonnet C, Walsh S, *et al*. 2012. Systems-based analysis of Arabidopsis leaf growth reveals adaptation to water deficit. Molecular Systems Biology **8,** 606.

Baker NR, Harbinson J, Kramer DM. 2007. Determining the limitations and regulation of photosynthetic energy transduction in leaves. Plant, Cell & Environment **30,** 1107–1125.

Bechtold U, Penfold CA, Jenkins DJ, *et al*. 2016. Time-series transcriptomics reveals that *AGAMOUS-LIKE22* affects primary metabolism and developmental processes in drought-stressed Arabidopsis. The Plant Cell **28,** 345–366.

Bernacchi CJ, VanLoocke A. 2015. Terrestrial ecosystems in a changing environment: a dominant role for water. Annual Review of Plant Biology **66,** 599–622.

Buckley TN, Adams MA. 2011. An analytical model of non-photorespiratory CO_2 release in the light and dark in leaves of C_3 species based on stoichiometric flux balance. Plant, Cell & Environment **34,** 89–112.

Carrillo LR, Froehlich JE, Cruz JA, Savage LJ, Kramer DM. 2016. Multi-level regulation of the chloroplast ATP synthase: the chloroplast NADPH thioredoxin reductase C (NTRC) is required for redox modulation specifically under low irradiance. The Plant Journal **87,** 654–663.

Chai TT, Simmonds D, Day DA, Colmer TD, Finnegan PM. 2012. A *GmAOX2b* antisense gene compromises vegetative growth and seed production in soybean. Planta **236,** 199–207.

Cheung CY, Ratcliffe RG, Sweetlove LJ. 2015. A method of accounting for enzyme costs in flux balance analysis reveals alternative pathways and metabolite stores in an illuminated Arabidopsis leaf. Plant Physiology **169,** 1671–1682.

Clauw P, Coppens F, De Beuf K, *et al*. 2015. Leaf responses to mild drought stress in natural variants of Arabidopsis. Plant Physiology **167,** 800–816.

Clifton R, Millar AH, Whelan J. 2006. Alternative oxidases in *Arabidopsis*: a comparative analysis of differential expression in the gene family provides new insights into function of non-phosphorylating bypasses. Biochimica et Biophysica Acta **1757,** 730–741.

Condon AG, Richards RA, Rebetzke GJ, Farquhar GD. 2002. Improving intrinsic water-use efficiency and crop yield. Crop Science **42,** 122–131.

Condon AG, Richards RA, Rebetzke GJ, Farquhar GD. 2004. Breeding for high water-use efficiency. Journal of Experimental Botany **55,** 2447–2460.

Cruz JA, Avenson TJ, Kanazawa A, Takizawa K, Edwards GE, Kramer DM. 2005. Plasticity in light reactions of photosynthesis for energy production and photoprotection. Journal of Experimental Botany **56,** 395–406.

Cruz JA, Sacksteder CA, Kanazawa A, Kramer DM. 2001. Contribution of electric field ($\Delta\psi$) to steady-state transthylakoid proton motive force (*pmf*) in vitro and in vivo. Control of *pmf* parsing into $\Delta\psi$ and ΔpH by ionic strength. Biochemistry **40,** 1226–1237.

Cvetkovska M, Dahal K, Alber NA, Jin C, Cheung M, Vanlerberghe GC. 2014. Knockdown of mitochondrial alternative oxidase induces the 'stress state' of signaling molecule pools in *Nicotiana tabacum*, with implications for stomatal function. New Phytologist **203,** 449–461.

Cvetkovska M, Vanlerberghe GC. 2012. Alternative oxidase modulates leaf mitochondrial concentrations of superoxide and nitric oxide. New Phytologist **195,** 32–39.

Dahal K, Martyn GD, Alber NA, Vanlerberghe GC. 2017. Coordinated regulation of photosynthetic and respiratory components is necessary to maintain chloroplast energy balance in varied growth conditions. Journal of Experimental Botany **68,** 657–671.

Dahal K, Martyn GD, Vanlerberghe GC. 2015. Improved photosynthetic performance during severe drought in *Nicotiana tabacum* overexpressing a nonenergy conserving respiratory electron sink. New Phytologist **208,** 382–395.

Dahal K, Vanlerberghe GC. 2017. Alternative oxidase respiration maintains both mitochondrial and chloroplast function during drought. New Phytologist **213,** 560–571.

Dahal K, Wang J, Martyn GD, Rahimy F, Vanlerberghe GC. 2014. Mitochondrial alternative oxidase maintains respiration and preserves photosynthetic capacity during moderate drought in *Nicotiana tabacum*. Plant Physiology **166,** 1560–1574.

De Block M, Van Lijsebettens M. 2011. Energy efficiency and energy homeostasis as genetic and epigenetic components of plant performance and crop productivity. Current Opinion in Plant Biology **14,** 275–282.

Farquhar GD, Sharkey TD. 1982. Stomatal conductance and photosynthesis. Annual Review of Plant Physiology **33,** 317–345.

Finnegan PM, Soole KL, Umbach AL. 2004. Alternative electron transport proteins in plants. In: **Day DA, Millar AH, Whelan J**, eds. Plant mitochondria: from genome to function. Dordrecht, The Netherlands: Kluwer Academic Publishers, 163–230.

Fiorani F, Umbach AL, Siedow JN. 2005. The alternative oxidase of plant mitochondria is involved in the acclimation of shoot growth at low temperature. A study of *Arabidopsis AOX1a* transgenic plants. Plant Physiology **139,** 1795–1805.

Flexas J, Bota J, Loreto F, Cornic G, Sharkey TD. 2004. Diffusive and metabolic limitations to photosynthesis under drought and salinity in C_3 plants. Plant Biology **6,** 269–279.

Florez-Sarasa ID, Bouma TJ, Medrano H, Azcon-Bieto J, Ribas-Carbo M. 2007. Contribution of the cytochrome and alternative pathways to growth respiration and maintenance respiration in *Arabidopsis thaliana*. Physiologia Plantarum **129,** 143–151.

Foyer CH, Neukermans J, Queval G, Noctor G, Harbinson J. 2012. Photosynthetic control of electron transport and the regulation of gene expression. Journal of Experimental Botany **63,** 1637–1661.

Foyer CH, Ruban AV, Noctor G. 2017. Viewing oxidative stress through the lens of oxidative signalling rather than damage. The Biochemical Journal **474,** 877–883.

Gago J, Douthe C, Florez-Sarasa I, Escalona JM, Galmes J, Fernie AR, Flexas J, Medrano H. 2014. Opportunities for improving leaf water use efficiency under climate change conditions. Plant Science **226,** 108–119.

Gardeström P, Igamberdiev AU. 2016. The origin of cytosolic ATP in photosynthetic cells. Physiologia Plantarum **157,** 367–379.

Genty B, Briantais J-M, Baker NR. 1989. The relationship between the quantum yield of photosynthetic electron transport and quenching of chlorophyll fluorescence. Biochimica et Biophysica Acta **990,** 87–92.

Gifford RM. 2003. Plant respiration in productivity models: conceptualisation, representation and issues for global terrestrial carbon-cycle research. Functional Plant Biology **30,** 171–186.

Grassi G, Magnani F. 2005. Stomatal, mesophyll conductance and biochemical limitations to photosynthesis as affected by drought and leaf ontogeny in ash and oak trees. Plant, Cell and Environment **28,** 834–849.

Harb A, Krishnan A, Ambavaram MM, Pereira A. 2010. Molecular and physiological analysis of drought stress in Arabidopsis reveals early responses leading to acclimation in plant growth. Plant Physiology **154,** 1254–1271.

Herdean A, Teardo E, Nilsson AK, *et al*. 2016. A voltage-dependent chloride channel fine-tunes photosynthesis in plants. Nature Communications **7,** 11654.

Hoefnagel MHN, Atkin OK, Wiskich JT. 1998. Interdependence between chloroplasts and mitochondria in the light and the dark. Biochimica et Biophysica Acta **1366,** 235–255.

Hoshiyasu S, Kohzuma K, Yoshida K, Fujiwara M, Fukao Y, Yokota A, Akashi K. 2013. Potential involvement of N-terminal acetylation in the quantitative regulation of the ε subunit of chloroplast ATP synthase under drought stress. Bioscience, Biotechnology, and Biochemistry **77,** 998–1007.

Hughes J, Hepworth C, Dutton C, Dunn JA, Hunt L, Stephens J, Waugh R, Cameron DD, Gray JE. 2017. Reducing stomatal density in barley improves drought tolerance without impacting on yield. Plant Physiology **174,** 776–787.

Hummel I, Pantin F, Sulpice R, *et al*. 2010. Arabidopsis plants acclimate to water deficit at low cost through changes of carbon usage: an integrated perspective using growth, metabolite, enzyme, and gene expression analysis. Plant Physiology **154,** 357–372.

Hüner NPA, Öquist G, Sarhan F. 1998. Energy balance and acclimation to light and cold. Trends in Plant Science **3,** 224–230.

Johnson GN. 2011. Physiology of PSI cyclic electron transport in higher plants. Biochimica et Biophysica Acta **1807,** 384–389.

Johnson MP, Ruban AV. 2014. Rethinking the existence of a steady-state $\Delta\psi$ component of the proton motive force across plant thylakoid membranes. Photosynthesis Research **119,** 233–242.

Kanazawa A, Kramer DM. 2002. *In vivo* modulation of nonphotochemical exciton quenching (NPQ) by regulation of the chloroplast ATP synthase. Proceedings of National Academy of Sciences, USA **99,** 12789–12794.

Karaba A, Dixit S, Greco R, *et al*. 2007. Improvement of water use efficiency in rice by expression of *HARDY*, an *Arabidopsis* drought and salt tolerance gene. Proceedings of the National Academy of Sciences, USA **104,** 15270–15275.

Kiirats O, Cruz JA, Edwards GE, Kramer DM. 2009. Feedback limitation of photosynthesis at high CO_2 acts by modulating the activity of the chloroplast ATP synthase. Functional Plant Biology **36,** 893–901.

Klughammer C, Schreiber U. 2008. Saturation pulse method for assessment of energy conversion in PSI. PAM Application Notes **1,** 11–14.

Kohzuma K, Cruz JA, Akashi K, Hoshiyasu S, Munekage YN, Yokota A, Kramer DM. 2009. The long-term responses of the photosynthetic proton circuit to drought. Plant, Cell & Environment **32,** 209–219.

Kohzuma K, Froehlich JE, Davis GA, Temple JA, Minhas D, Dhingra A, Cruz JA, Kramer DM. 2017. The role of light-dark regulation of the chloroplast ATP synthase. Frontiers in Plant Science **8,** 1248.

Kramer DM, Cruz JA, Kanazawa A. 2003. Balancing the central roles of the thylakoid proton gradient. Trends in Plant Science **8,** 27–32.

Kramer DM, Evans JR. 2011. The importance of energy balance in improving photosynthetic productivity. Plant Physiology **155,** 70–78.

Kramer DM, Johnson G, Kiirats O, Edwards GE. 2004. New fluorescence parameters for the determination of Q_A redox state and excitation energy fluxes. Photosynthesis Research **79,** 209.

Krömer S. 1995. Respiration during photosynthesis. Annual Review of Plant Physiology and Plant Molecular Biology **46,** 45–70.

Lawlor DW. 2002. Limitation of photosynthesis in water-stressed leaves: stomata *vs*. metabolism and the role of ATP. Annals of Botany **89,** 871–885.

Lawlor DW. 2013. Genetic engineering to improve plant performance under drought: physiological evaluation of achievements, limitations, and possibilities. Journal of Experimental Botany **64,** 83–108.

Lawlor DW, Tezara W. 2009. Causes of decreased photosynthetic rate and metabolic capacity in water-deficient leaf cells: a critical evaluation of mechanisms and integration of processes. Annals of Botany **103,** 561–579.

Liu YJ, Nunes-Nesi A, Wallström SV, *et al*. 2009. A redox-mediated modulation of stem bolting in transgenic *Nicotiana sylvestris* differentially expressing the external mitochondrial NADPH dehydrogenase. Plant Physiology **150,** 1248–1259.

Mahler H, Wuennenberg P, Linder M, Przybyla D, Zoerb C, Landgraf F, Forreiter C. 2007. Singlet oxygen affects the activity of the thylakoid ATP synthase and has a strong impact on its gamma subunit. Planta **225,** 1073–1083.

Masle J, Gilmore SR, Farquhar GD. 2005. The *ERECTA* gene regulates plant transpiration efficiency in *Arabidopsis*. Nature **436,** 866–870.

Mathy G, Cardol P, Dinant M, *et al*. 2010. Proteomic and functional characterization of a *Chlamydomonas reinhardtii* mutant lacking the mitochondrial alternative oxidase 1. Journal of Proteome Research **9,** 2825–2838.

Maxwell DP, Wang Y, McIntosh L. 1999. The alternative oxidase lowers mitochondrial reactive oxygen production in plant cells. Proceedings of the National Academy of Sciences, USA **96,** 8271–8276.

Maxwell K, Johnson GN. 2000. Chlorophyll fluorescence—a practical guide. Journal of Experimental Botany **51,** 659–668.

Millar AH, Atkin OK, Ian Menz R, Henry B, Farquhar G, Day DA. 1998. Analysis of respiratory chain regulation in roots of soybean seedlings. Plant Physiology **117,** 1083–1093.

Millar AH, Whelan J, Soole KL, Day DA. 2011. Organization and regulation of mitochondrial respiration in plants. Annual Review of Plant Biology **62,** 79–104.

Millenaar FF, Gonzàlez-Meler MA, Fiorani F, Welschen R, Ribas-Carbo M, Siedow JN, Wagner AM, Lambers H. 2001. Regulation of alternative oxidase activity in six wild monocotyledonous species. An *in vivo* study at the whole root level. Plant Physiology **126,** 376–387.

Nikoloski Z, Perez-Storey R, Sweetlove LJ. 2015. Inference and prediction of metabolic network fluxes. Plant Physiology **169,** 1443–1455.

Noctor G, De Paepe R, Foyer CH. 2007. Mitochondrial redox biology and homeostasis in plants. Trends in Plant Science **12,** 125–134.

Noctor G, Mhamdi A, Foyer CH. 2014. The roles of reactive oxygen metabolism in drought: not so cut and dried. Plant Physiology **164,** 1636–1648.

Noguchi K, Yoshida K. 2008. Interaction between photosynthesis and respiration in illuminated leaves. Mitochondrion **8,** 87–99.

Nunes-Nesi A, Araújo WL, Fernie AR. 2011. Targeting mitochondrial metabolism and machinery as a means to enhance photosynthesis. Plant Physiology **155,** 101–107.

Oelze ML, Kandlbinder A, Dietz KJ. 2008. Redox regulation and overreduction control in the photosynthesizing cell: complexity in redox regulatory networks. Biochimica et Biophysica Acta **1780,** 1261–1272.

Perez-Martin A, Michelazzo C, Torres-Ruiz JM, Flexas J, Fernández JE, Sebastiani L, Diaz-Espejo A. 2014. Regulation of photosynthesis and stomatal and mesophyll conductance under water stress and recovery in olive trees: correlation with gene expression of carbonic anhydrase and aquaporins. Journal of Experimental Botany **65,** 3143–3156.

Pinheiro C, Chaves MM. 2011. Photosynthesis and drought: can we make metabolic connections from available data? Journal of Experimental Botany **62,** 869–882.

Plaxton WC, Podestá FE. 2006. The functional organization and control of plant respiration. Critical Reviews in Plant Science **25,** 159–198.

Polley HW. 2002. Implications of atmospheric and climatic change for crop yield and water use efficiency. Crop Science **42,** 131–140.

Raghavendra AS, Padmasree K. 2003. Beneficial interactions of mitochondrial metabolism with photosynthetic carbon assimilation. Trends in Plant Science **8,** 546–553.

Rivero RM, Shulaev V, Blumwald E. 2009. Cytokinin-dependent photorespiration and the protection of photosynthesis during water deficit. Plant Physiology **150,** 1530–1540.

Rott M, Martins NF, Thiele W, Lein W, Bock R, Kramer DM, Schöttler MA. 2011. ATP synthase repression in tobacco restricts photosynthetic electron transport, CO_2 assimilation, and plant growth by overacidification of the thylakoid lumen. The Plant Cell **23,** 304–321.

Schmidt C, Beilsten-Edmands V, Mohammed S, Robinson CV. 2017. Acetylation and phosphorylation control both local and global stability of the chloroplast F_1 ATP synthase. Scientific Reports **7,** 44068.

Schöttler MA, Tóth SZ. 2014. Photosynthetic complex stoichiometry dynamics in higher plants: environmental acclimation and photosynthetic flux control. Frontiers in Plant Science **5,** 188.

Schöttler MA, Tóth SZ, Boulouis A, Kahlau S. 2015. Photosynthetic complex stoichiometry dynamics in higher plants: biogenesis, function, and turnover of ATP synthase and the cytochrome b_6f complex. Journal of Experimental Botany **66,** 2373–2400.

Schreiber U, Klughammer C. 2008. New accessory for the DUAL-PAM-100: The P515/535 module and examples of its application. PAM Application Notes **1,** 1–10.

Shikanai T, Yamamoto H. 2017. Contribution of cyclic and pseudo-cyclic electron transport to the formation of proton motive force in chloroplasts. Molecular Plant **10,** 20–29.

Sieger SM, Kristensen BK, Robson CA, Amirsadeghi S, Eng EW, Abdel-Mesih A, Møller IM, Vanlerberghe GC. 2005. The role of alternative oxidase in modulating carbon use efficiency and growth during macronutrient stress in tobacco cells. Journal of Experimental Botany **56,** 1499–1515.

Skirycz A, De Bodt S, Obata T, *et al*. 2010. Developmental stage specificity and the role of mitochondrial metabolism in the response of Arabidopsis leaves to prolonged mild osmotic stress. Plant Physiology **152,** 226–244.

Stitt M, Lunn J, Usadel B. 2010. Arabidopsis and primary photosynthetic metabolism – more than the icing on the cake. The Plant Journal **61,** 1067–1091.

Takeno K. 2016. Stress-induced flowering: the third category of flowering response. Journal of Experimental Botany **67,** 4925–4934.

Taniguchi M, Miyake H. 2012. Redox-shuttling between chloroplast and cytosol: integration of intra-chloroplast and extra-chloroplast metabolism. Current Opinion in Plant Biology **15,** 252–260.

Tcherkez G, Boex-Fontvieille E, Mahé A, Hodges M. 2012. Respiratory carbon fluxes in leaves. Current Opinion in Plant Biology **15,** 308–314.

Tezara W, Mitchell V, Driscoll SP, Lawlor DW. 2002. Effects of water deficit and its interaction with CO_2 supply on the biochemistry and physiology of photosynthesis in sunflower. Journal of Experimental Botany **53,** 1781–1791.

Tezara W, Mitchell VJ, Driscoll SD, Lawlor DW. 1999. Water stress inhibits plant photosynthesis by decreasing coupling factor and ATP. Nature **401,** 914–917.

Thompson AJ, Andrews J, Mulholland BJ, *et al*. 2007. Overproduction of abscisic acid in tomato increases transpiration efficiency and root hydraulic conductivity and influences leaf expansion. Plant Physiology **143,** 1905–1917.

Tikhonov AN. 2013. pH-dependent regulation of electron transport and ATP synthesis in chloroplasts. Photosynthesis Research **116,** 511–534.

Tikhonov AN. 2014. The cytochrome b_6f complex at the crossroad of photosynthetic electron transport pathways. Plant Physiology and Biochemistry **81,** 163–183.

Vanlerberghe GC. 2013. Alternative oxidase: a mitochondrial respiratory pathway to maintain metabolic and signaling homeostasis during abiotic and biotic stress in plants. International Journal of Molecular Sciences **14,** 6805–6847.

Vanlerberghe GC, Day DA, Wiskich JT, Vanlerberghe AE, McIntosh L. 1995. Alternative oxidase activity in tobacco leaf mitochondria (dependence on tricarboxylic acid cycle-mediated redox regulation and pyruvate activation). Plant Physiology **109,** 353–361.

von Caemmerer S, Farquhar GD. 1981. Some relationships between the biochemistry of photosynthesis and the gas exchange of leaves. Planta **153,** 376–387.

Wang J, Rajakulendran N, Amirsadeghi S, Vanlerberghe GC. 2011. Impact of mitochondrial alternative oxidase expression on the response of *Nicotiana tabacum* to cold temperature. Physiologia Plantarum **142,** 339–351.

Wang J, Vanlerberghe GC. 2013. A lack of mitochondrial alternative oxidase compromises capacity to recover from severe drought stress. Physiologia Plantarum **149,** 461–473.

Weraduwage SM, Chen J, Anozie FC, Morales A, Weise SE, Sharkey TD. 2015. The relationship between leaf area growth and biomass accumulation in *Arabidopsis thaliana*. Frontiers in Plant Science **6,** 167.

Wilson KE, Ivanov AG, Öquist G, Grodzinski B, Sarhan F, Hüner NPA. 2006. Energy balance, organellar redox status, and acclimation to environmental stress. Canadian Journal of Botany **84,** 1355–1370.

Wobbe L, Bassi R, Kruse O. 2016. Multi-level light capture control in plants and green algae. Trends in Plant Science **21,** 55–68.

Yamori W, Evans JR, Von Caemmerer S. 2010. Effects of growth and measurement light intensities on temperature dependence of CO_2 assimilation rate in tobacco leaves. Plant, Cell & Environment **33,** 332–343.

Yamori W, Sakata N, Suzuki Y, Shikanai T, Makino A. 2011*a*. Cyclic electron flow around photosystem I via chloroplast NAD(P)H dehydrogenase (NDH) complex performs a significant physiological role during photosynthesis and plant growth at low temperature in rice. The Plant Journal **68,** 966–976.

Yamori W, Takahashi S, Makino A, Price GD, Badger MR, von Caemmerer S. 2011*b*. The roles of ATP synthase and the cytochrome b_6/f complexes in limiting chloroplast electron transport and determining photosynthetic capacity. Plant Physiology **155,** 956–962.

Yang JT, Preiser AL, Li Z, Weise SE, Sharkey TD. 2016*a*. Triose phosphate use limitation of photosynthesis: short-term and long-term effects. Planta **243,** 687–698.

Yang Z, Liu J, Tischer SV, Christmann A, Windisch W, Schneyder H, Grill E. 2016*b*. Leveraging abscisic acid receptors for efficient water use in *Arabidopsis*. Proceedings of the National Academy of Sciences, USA **113,** 6791–6796.

Yu H, Chen X, Hong YY, *et al*. 2008. Activated expression of an *Arabidopsis* HD-START protein confers drought tolerance with improved root system and reduced stomatal density. The Plant Cell **20,** 1134–1151.

Zhou S, Medlyn B, Sabaté S, Sperlich D, Prentice IC. 2014. Short-term water stress impacts on stomatal, mesophyll and biochemical limitations to photosynthesis differ consistently among tree species from contrasting climates. Tree Physiology **34,** 1035–1046.

Zidenga T, Leyva-Guerrero E, Moon H, Siritunga D, Sayre R. 2012. Extending cassava root shelf life via reduction of reactive oxygen species production. Plant Physiology **159,** 1396–1407.